

Determination of effective trapping times for electrons and holes in irradiated silicon

G. Kramberger ¹, V. Cindro, I. Mandić, M. Mikuz, M. Zavrtanik

*Institute Jožef Stefan and Department of Physics,
University of Ljubljana, SI-1000 Ljubljana, Slovenia*

Abstract

A set of standard and oxygenated silicon diodes with different resistivities ($1 \text{ k}\Omega\text{cm}$ and $15 \text{ k}\Omega\text{cm}$) was irradiated with neutrons to fluences up to $2 \times 10^{14} \text{ cm}^{-2}$. 1 MeV neutron NIEL equivalent. After beneficial annealing the signal response from the diodes was studied using TCT (transient current technique). Red laser ($\lambda=670 \text{ nm}$) illumination was used for creation of electrons and holes.

Assuming exponential decrease of the drifting charge in time, the effective trapping probability of electrons and holes was deduced from the evolution of the induced current at voltages above the full depletion voltage. The effective trapping probabilities of holes were found to be larger than for electrons. The trapping probability is shown to scale linearly with fluence. No significant difference between effective trapping probabilities for different materials was measured.

PACS: 85.30.De; 29.40.Wk; 29.40.Gx

Key words: Effective trapping time, Silicon detectors, Charge collection efficiency, LHC detectors

1 Introduction

Experiments at LHC will extensively use silicon microstrip detectors for tracking of charged particles. High luminosity and large proton-proton inelastic cross section will result in intense fluxes of heavy particles to which silicon detectors will be exposed. As an example the ATLAS Semiconductor Tracker

¹ Corresponding author; Address: Jožef Stefan Institute, Jamnova 39, SI-1000 Ljubljana, Slovenia. Tel: (+386) 1 4773512, fax: (+386) 1 4257074, e-mail: Gregor.Kramberger@ijs.si

will be exposed to fluences up to $1.5 \times 10^{14} \text{ cm}^{-2}$ 1 MeV neutron non-ionizing energy loss (NIEL) equivalent. Radiation damage in silicon will cause changes in the full depletion voltage (FDV) and an increase of leakage current, as well as trapping of the drifting charge. The dynamics of defects and the related change of effective doping concentration and leakage current with time have been extensively studied [1].

Measurements of the effective trapping probability responsible for a decrease of the charge collection efficiency (CCE), are, on the other hand, much more scarce. Most methods used for the determination of effective trapping times are based on measurements of time-resolved current pulse shapes in silicon detectors. The previous measurements of effective trapping times were either limited to low fluences [2] or relied on the knowledge of the electric field [3]. Here we present the results of a new method for the determination of effective trapping times using the transient current technique (TCT).

The experimental setup, details on the method and results with different silicon materials are presented and discussed in the following sections.

2 Setup

Free carriers created in the active region of a reverse biased silicon detector experience drift in the electric field, thus giving rise to the current induced on both electrodes of the detector.

In our case, hole-electron pairs were created by a red laser pulse ($\lambda = 670 \text{ nm}$). The majority of electron-hole pairs was created in the close proximity of the detector surface since the penetration depth for the red light used is $\alpha^{-1} = 3.3 \text{ } \mu\text{m}$ at $T = 293 \text{ K}$.

After the creation of electron-hole pairs in the direct vicinity of the detector electrode, electrons (p -side illumination) and holes (n -side illumination), respectively, drift through the entire depth of the detector. Accordingly, the complementary charge carriers are collected immediately by the adjacent electrode thus contributing negligibly to the induced current. In this way, it is possible to distinguish between hole and electron signals.

A good time resolution was obtained by the short laser pulse ($FWHM \sim 1.4 \text{ ns}$) generating approximately $5 \cdot 10^5$ pairs. An optical transport system was used for attenuation and focusing of the laser beam. The minimal spot size has a diameter of $\sim 100 \text{ } \mu\text{m}$. The detectors were put in a LN₂ pour fill optical cryostat which allowed a stable ($\pm 0.2 \text{ K}$) temperature in the range from 77 K - 300 K.

The induced current was amplified with a fast current amplifier (bandwidth 0.01-1 GHz, amplification 55 dB) and subsequently digitized with a 500 MHz digital oscilloscope. The data were transferred to the computer, deconvoluted to correct for the electronic transfer function of the readout and analyzed.

2.1 Samples

In this study several $p^+ - n - n^+$ pad detectors processed on high (15 k Ω cm) and low resistivity (1 k Ω cm) standard and oxygen enriched silicon wafers were irradiated with neutrons to fluences up to $\Phi_{\text{eq}} = 2 \cdot 10^{14} / \text{cm}^2$ 1 MeV neutron NIEL equivalent. The diodes produced on high resistivity wafers were processed by ST Microelectronics while the the low resistivity ones were processed at Brookhaven National Laboratory (see Table 1).

Sample name	Producer (wafer)	Oxygenation (h)	Initial resistivity	Φ_{eq} [10^{13} n/cm 2]	FDV [V] non-irr.
W3397	STM (Wacker)	no	15 k Ω cm	0	15
W3398	STM (Wacker)	no	15 k Ω cm	2.5	12
W3391	STM (Wacker)	no	15 k Ω cm	5	16
W33911	STM (Wacker)	no	15 k Ω cm	7.5	14
W3392	STM (Wacker)	no	15 k Ω cm	10	13
W3393	STM (Wacker)	no	15 k Ω cm	15	12
W3394	STM (Wacker)	no	15 k Ω cm	20	13
W3178	STM (Wacker)	60	15 k Ω cm	2.5	19
W31711	STM (Wacker)	60	15 k Ω cm	7.5	18
VZ10	BNL (Topsil)	no	≈ 1 k Ω cm	10	170
VZ9	BNL (Topsil)	no	≈ 1 k Ω cm	20	210
VZ7	BNL (Topsil)	12	≈ 1 k Ω cm	10	250
VZ5	BNL (Topsil)	12	≈ 1 k Ω cm	20	250

Table 1

The samples used in the study. The oxygenated samples were first kept in an O $_2$ atmosphere and then in N $_2$.

The diodes had a hole ($\phi = 2$ mm) in the metalization on the p^+ side for light injection, while on the n^+ side a mesh metalization was used for the same purpose. The irradiation of the diodes took place in the TRIGA nuclear reactor at the Jožef Stefan Institute. The accuracy of fluences is estimated

to be about 10% [4]. During and after the irradiation the diodes were kept unbiased. After the irradiation they were mounted to an aluminum support, glued and annealed at room temperature (RT) to the minimum in FDV. The evolution of the FDV was measured with the *CV* method at a frequency $\nu = 10$ kHz and $T = 20^\circ$ C. The minimum values of the FDV are shown in Fig. 1. Once the diodes reached the minimum in FDV they were stored at $T = -17^\circ$ C.

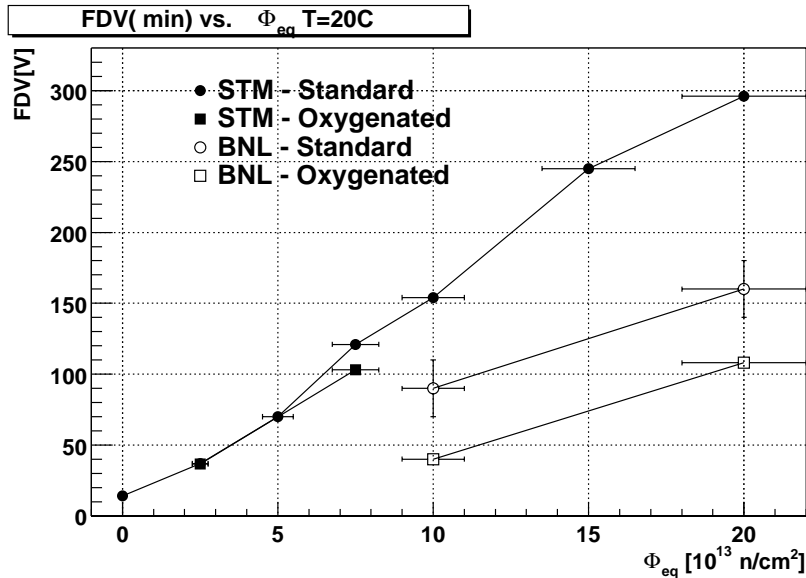


Fig. 1. The FDV as measured with the *CV* method in the minimum after the irradiation. The FDV of the samples VZ10 and VZ9 has a larger uncertainty due to non-ideal *CV* characteristics.

3 Determination of the effective trapping probability

3.1 Method

The measured charge in an unirradiated detector reaches a plateau at voltages exceeding FDV, provided the current integration time is longer than the drift time of electrons and holes.

During the drift through an irradiated detector a part of the drifting charge is trapped at radiation-induced traps. An increase of drift velocity due to the higher field at voltages above FDV reduces the drift time of the charge and by that the amount of the charge being trapped. If the integration time of the induced current is large enough, all the trapped charge is detrapped and the collected charge (current integral) saturates at voltages above FDV. At

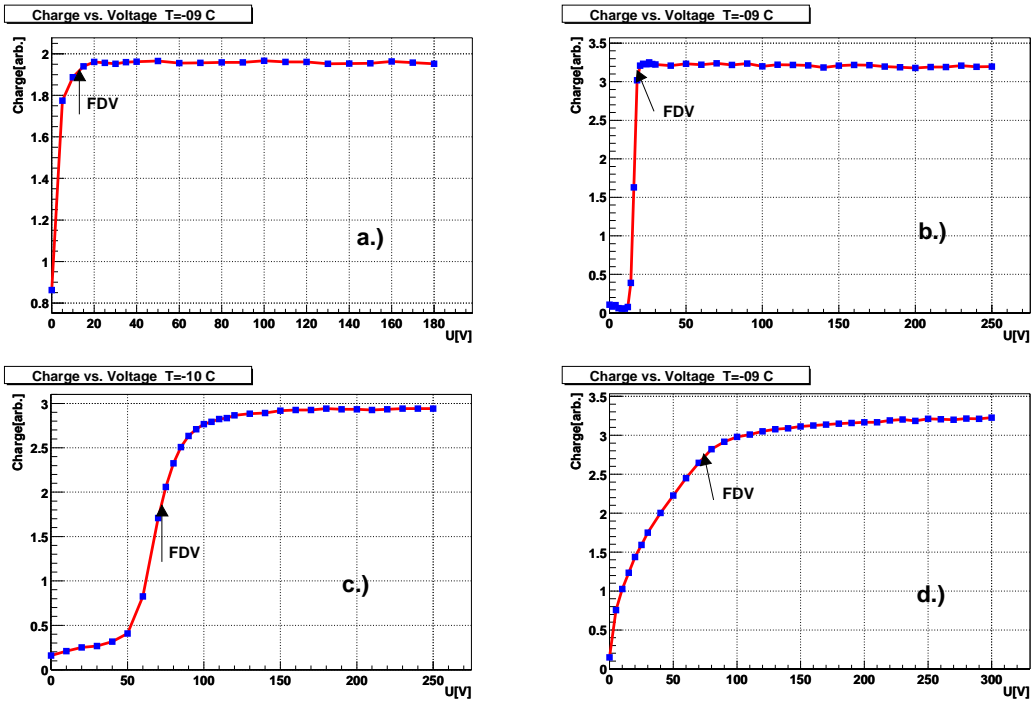


Fig. 2. Measured charge integrated over 60 ns after the electron injection a.) and hole injection b.) in the sample W3397. Same for the sample W3391: c.) electron injection and d.) hole injection. For the W3391 The measured charge does not saturate at voltages above FDV. The y-axis unit corresponds to $\approx 3 \cdot 10^5$ e-h pairs.

LHC, however, a short bunch crossing time (BCT=25 ns) and a large number of created particles require short shaping times of readout electronics in order to relate signals with the corresponding bunch crossing. Since the detrapping times are much longer than BCT, the charge once trapped is lost for the measurement [6].

The induced current from an instant hole or electron injection in the diode is given by Ramo's theorem [5] as

$$I(t)_{e,h} = e_0 N_{e,h}(t) \frac{1}{D} v_{e,h}(t) \quad , \quad (1)$$

with e_0 the unit charge, $N_{e,h}(t)$ the number of drifting electrons and holes, respectively, D the detector thickness, and $v_{e,h}$ the drift velocity. The amount of the drifting charge decreases with time due to trapping as

$$N_{e,h}(t) = N_{e,h}(0) \exp\left(\frac{-t}{\tau_{eff_{e,h}}}\right) \quad , \quad (2)$$

where $N_{e,h}(0)$ is the number of generated electron-hole pairs and $1/\tau_{eff_{e,h}}$ the

effective trapping probability defined as

$$\frac{1}{\tau_{eff_{e,h}}} = \sum_t N_t (1 - P_t^{e,h}) \sigma_{t_{e,h}} v_{th_{e,h}}(T) \quad (3)$$

where N_t denotes the concentration of the defect responsible for the trapping, $P_t^{e,h}$ its occupation probability with the relevant carrier, $v_{th_{e,h}}(T)$ the thermal velocity of drifting carriers and the $\sigma_{t_{e,h}}$ the carrier capture cross-section. The sum runs over all defects.

The effective trapping time can be determined by observing the behavior of the current integral at voltages above FDV. From Eqs. (2) and (1) it can be seen that correcting the measured $I_m(t)$ with a single exponential can compensate for trapping (Fig. 3), provided that the laser pulse is short compared to the drift time

$$I_c(t) = I_m(t) \exp\left(\frac{t - t_0}{\tau_{tr}}\right) \quad (4)$$

Here t_0 is the carrier injection time, in our case set to the start of the laser pulse.

If τ_{tr} in Eq. (4) represents the correct effective trapping time then the integral over time is equal for all voltages above FDV (Fig. 4). At voltages below FDV the correction of current shapes cannot be done in a simple way. Therefore the method was applied at voltages above FDV only. The ratio of measured and corrected charge represents the charge collection efficiency.

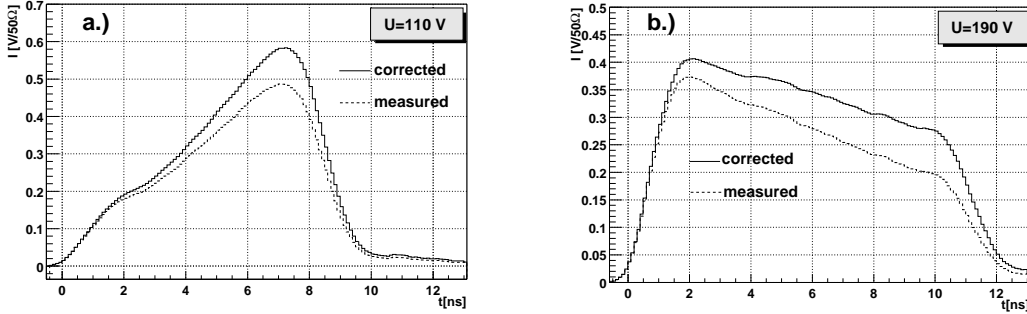


Fig. 3. Measured and corrected induced current shapes for the sample W3391: a.) electrons and b.) holes .

An example of extracting the effective trapping probability for electrons is shown in Fig. 4. If $1/\tau_{tr} > 1/\tau_{eff_{e,h}}$ the corrected charge is too high at low voltages where the charge drift is long and vice versa for $1/\tau_{tr} < 1/\tau_{eff_{e,h}}$. If $1/\tau_{tr} = 1/\tau_{eff_{e,h}}$ the corrected charge does not depend on voltage. The slope of the linear fit to the corrected charge as a function of voltage thus changes

sign at $1/\tau_{tr} = 1/\tau_{eff_{e,h}}$. In Fig. 5 an example of finding the effective trapping

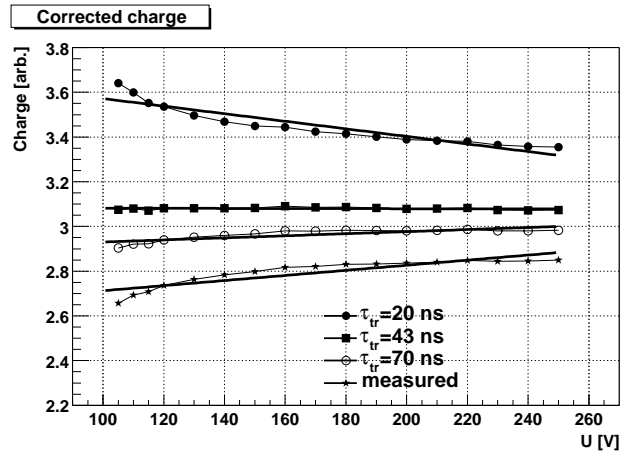


Fig. 4. Measured charge and charge corrected with different τ_{tr} .

probability is shown.

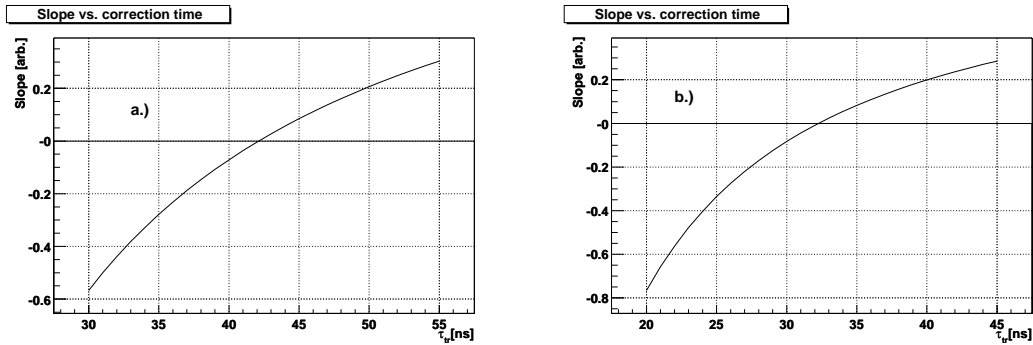


Fig. 5. The slope of the linear fit to the corrected charge vs. voltage as a function of τ_{tr} for W3391: a.) electrons and b.) holes. The effective trapping probability is determined from the zero intersection point.

The uncertainty of this method comes from the variation of the slope given by the fit. The later is related to the number of points included in the fit. The average error was estimated to 10% of the effective trapping time by changing fit intervals on different samples. In order to check the reproducibility the W3391 diode was mounted, measured and dismantled from the cryostat several times. The measured effective trapping times were always equal within 10%.

3.2 Results

The effective trapping probability for electrons and holes can be seen in Fig. 3.2. The measurements were done at $T = 263$ K close to the operation tem-

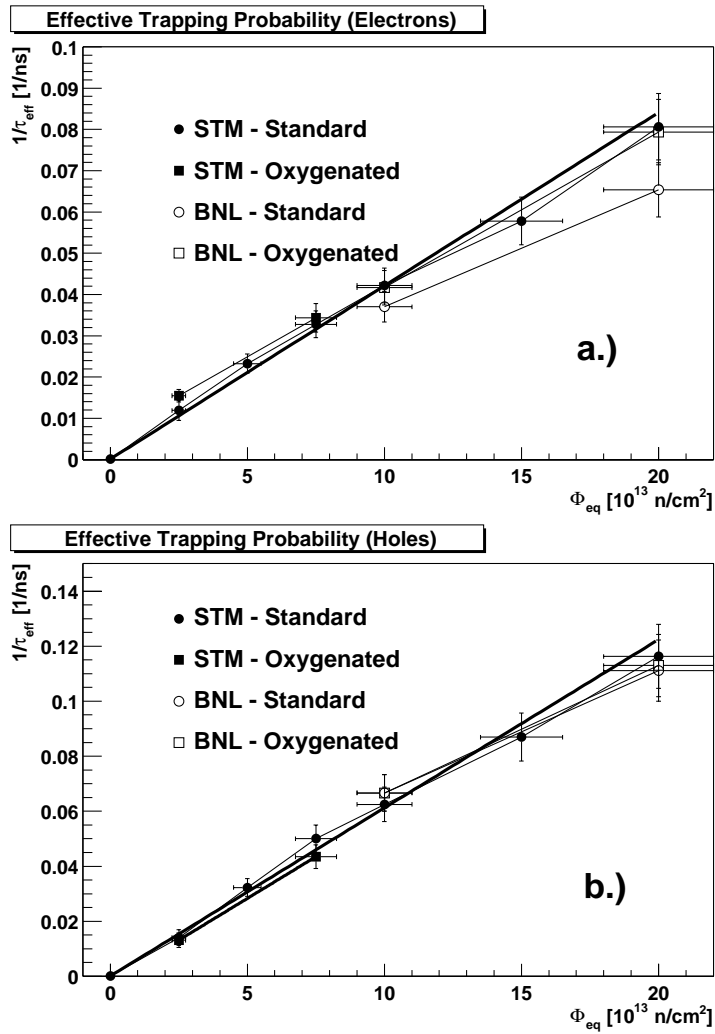


Fig. 6. The effective trapping probability measured at $T = 263$ K in different materials for: a.) electrons and b.) holes .

perature of silicon detectors at LHC. A linear dependence on fluence can be observed:

$$\frac{1}{\tau_{\text{eff},e,h}} = \beta_{e,h} \Phi_{\text{eq}}, \quad (5)$$

with

$$\beta_e = (4.2 \pm 0.3) 10^{-16} \text{ cm}^2/\text{ns} \quad \text{and} \quad \beta_h = (6.1 \pm 0.3) 10^{-16} \text{ cm}^2/\text{ns}.$$

This is in agreement with Eq. (3), as the trap concentration N_t is expected to increase linearly with fluence. Contrary to results of previous measurements [2,3] the effective trapping probability of holes is found to be about 50% larger than that of electrons. While the measured effective trapping probability for electrons is in agreement with [2] within the error, our effective trapping prob-

ability for holes is approximately two times larger.

No difference between oxygenated and non-oxygenated material can be observed. The initial resistivity also has no effect on the effective trapping probability.

4 CCE reduction due to trapping for minimum ionizing particles

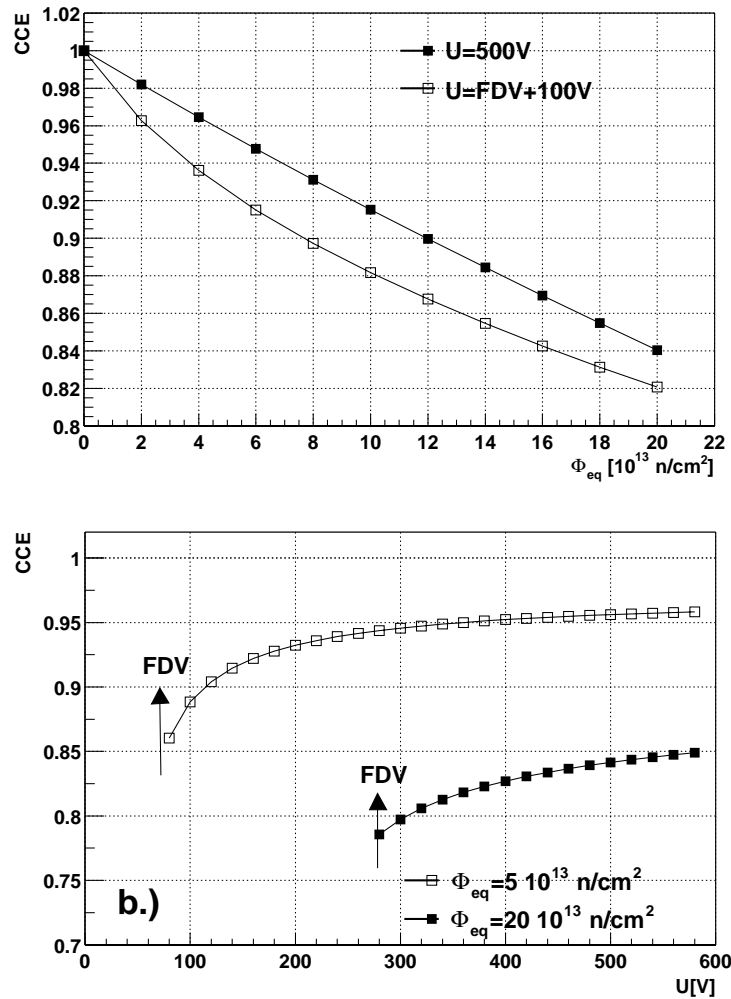


Fig. 7. Simulated CCE for an irradiated diode at $T = 263$ K for the case of constant bias $U = 500$ V and $U = FDV + 100$ V a.). The CCE dependence on voltage at two different fluences b.).

The measured effective trapping probabilities were used as input for a simulation of the current induced by the charge generated by a minimum ionizing particle traversing the diode. A uniform deposition of the generated charge along the track was assumed. The generated charge was split into buckets

1 μm apart. The contribution of each bucket to the total electron or hole current was calculated according to Eq. (1). The drift velocity was taken as $v_{e,h} = \mu_{e,h} E$ with the mobility parameterization taken from [7]. The electric field E was calculated from Poisson's equation assuming uniform effective acceptor concentration obtained from $|N_{eff}| = g_c \Phi_{eq}$, with $g_c = 0.02 \text{ cm}^{-1}$. The FDV is connected to $|N_{eff}|$ via $\text{FDV} = \frac{e_0 |N_{eff}| D^2}{2\epsilon\epsilon_0}$.

The total current was damped with an exponential (Eq. (3)) to account for trapping. Finally the total electron and hole currents were summed and integrated. The charge collection efficiency was defined as the ratio between the current integrated with trapping included and the current integrated without trapping.

The simulated CCE as a function of voltage (Fig. 7a) is in agreement with measurements in [6,8]. The advantage from applying a bias voltage exceeding the FDV can be clearly seen (Fig. 7b). About 15 % of the charge is lost at fluences around $\Phi_{eq} = 2 \cdot 10^{14} \text{ n/cm}^2$ event with the detector biased to 500V. CCE decreases at lower bias and at $\text{FDV} = 280 \text{ V}$ drops to under 80%.

5 Conclusions

A set of diodes fabricated on different silicon materials was irradiated to fluences up to $2 \cdot 10^{14} \text{ n/cm}^2$, annealed to the minimum in FDV and measured with TCT. Measurements of the effective trapping times for electrons and holes were performed using the charge correction method. The effective trapping probability for both, electrons and holes, was found to increase linearly with fluence $1/\tau_{eff_{e,h}} = \beta_{e,h} \Phi_{eq}$. The value of the slope β at $T=263\text{K}$ is $\beta_e = (4.2 \pm 0.3) 10^{-16} \text{ cm}^2/\text{ns}$ and $\beta_h = (6.1 \pm 0.3) 10^{-16} \text{ cm}^2/\text{ns}$. No material dependence of the effective trapping probability was observed.

6 Acknowledgments

The authors would like to thank B. Dezillie and Z. Li for providing the BNL samples and to the ROSE collaboration, especially M. Moll, for the STM samples. We have also benefitted from fruitful discussions with A. Chilingarov.

References

- [1] G. Lindström et. al, Nuclear Instr. and Meth. A426 (1999) 1.

- [2] H.W. Kraner et al., Nuclear Instr. and Meth. A326 (1993) 350.
- [3] C. Leroy et al., Nuclear Instr. and Meth. A426 (1999) 99.
- [4] D. Žontar et al., Nuclear Instr. and Meth. A426 (1999) 51.
- [5] S. Ramo, Proc. IRE 27 (1939) 584.
- [6] V. Cindro et al., Nuclear Instr. and Meth. A439 (2000) 337.
- [7] S. Selberherr, W. Hansch, M. Seavey, and J. Slotboom., *The Evolution of the MINIMOS Mobility Model. Solid-State Electron.*, 33(11):1425–1436, 1990.
- [8] S.J. Bates et al., Nuclear Instr. and Meth. A379 (1996) 116.